Submitted to ADVANCED FUNCTIONAL MATERIALS

DOI: 10.1002/adfm.201202215.

Matrix Metalloproteinase Responsive, Proximity-activated Polymeric Nanoparticles for siRNA Delivery

By *Hongmei Li, Shann S. Yu, Martina Miteva, Christopher E. Nelson, Thomas Werfel, Todd D. Giorgio*, Craig L. Duvall**

Supporting Information

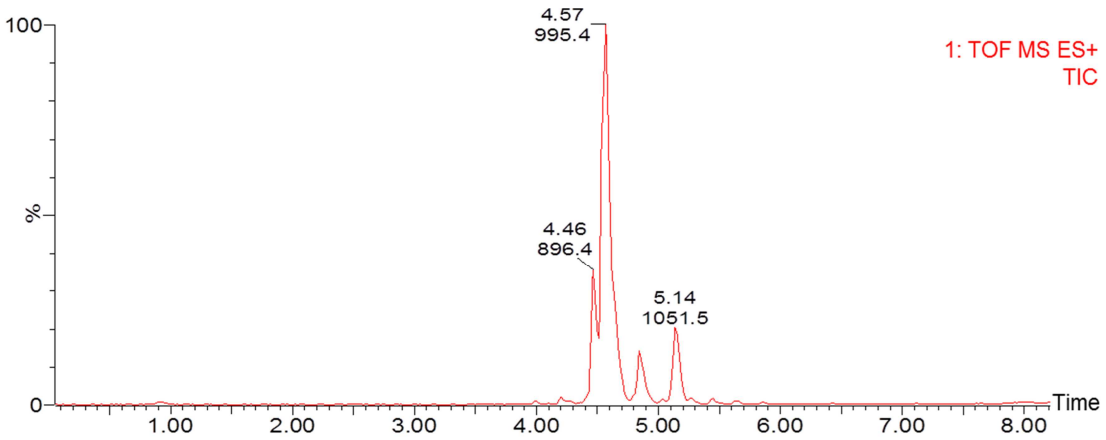

Figure S1. LC-MS analysis of the crude peptide prepared by solid phase peptide synthesis. The major peak at 4.57 min elution time (MW = 995.4 Da) is consistent with the estimated product molecular weight of 995 Da.

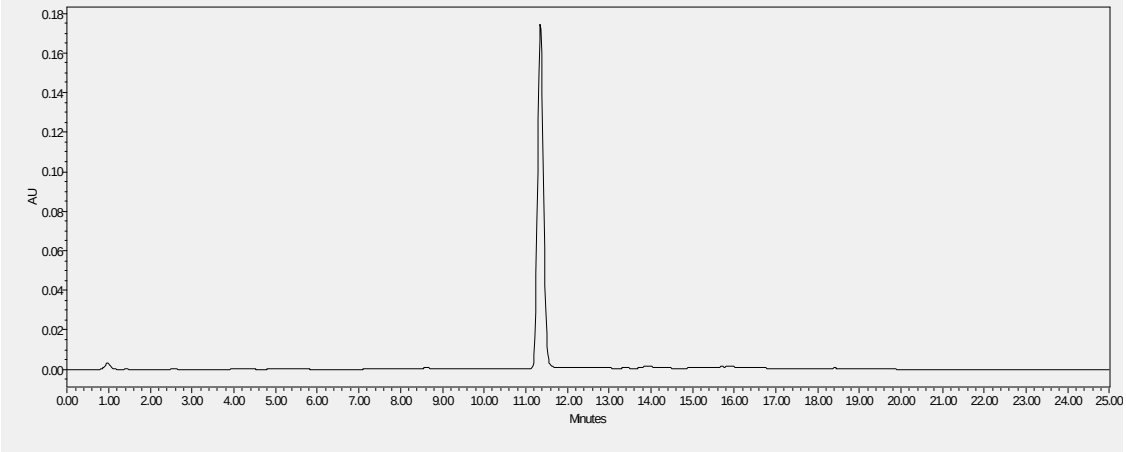

Figure S2. HPLC analysis of the purified peptide with reverse phase C18 column. Chromatography was monitored with UV-vis detector at 280 nm.

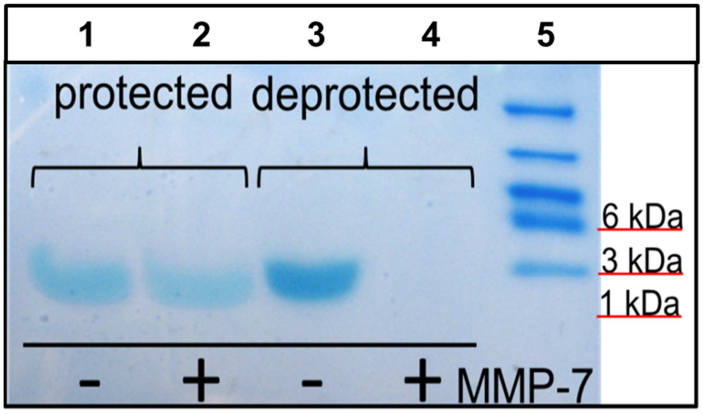

Figure S3. MMP-7 dependent cleavage of VPLSLYSGCG peptide. *t*-butyl protecting groups on amino acid side chains of the peptide (protected, lanes 1 and 2) inhibit MMP-7 proteolysis. Deprotected peptide was MMP-7 sensitive (lane 4), qualitatively confirmed by the absence of a band at the peptide MW relative to untreated control (lane 3).

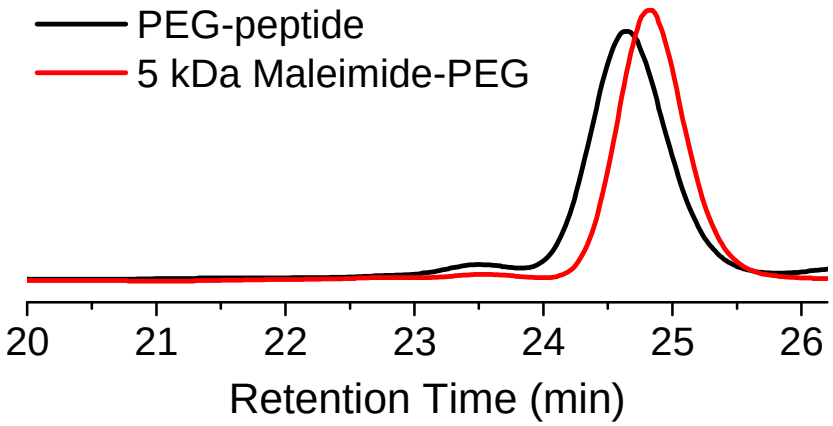

Figure S4. GPC confirmation of the 5 kDa maleimide end-functionalized PEG conjugation with the VPLSLYSGCG peptide.

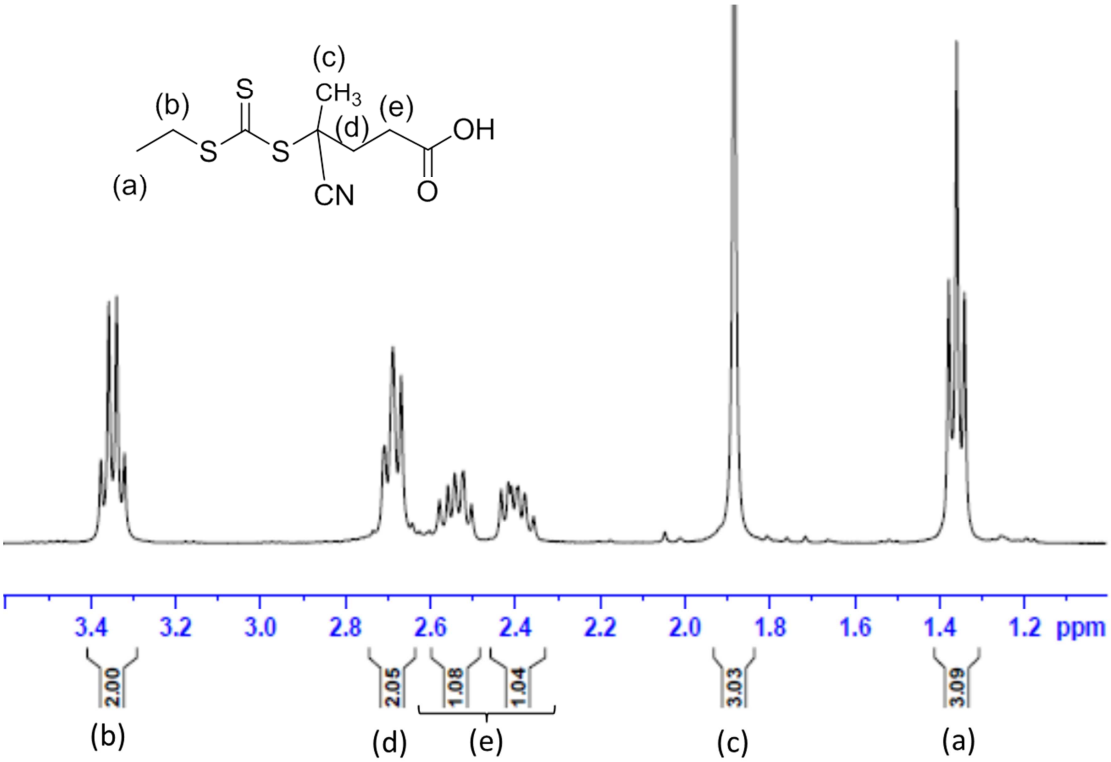

Figure S5. ^{1}H-NMR spectrum of the RAFT chain transfer agent, 4-cyano-4 (ethylsulfanylthio-carbonyl) sulfanylpentanoic acid (ECT) in $CDCl_3$.

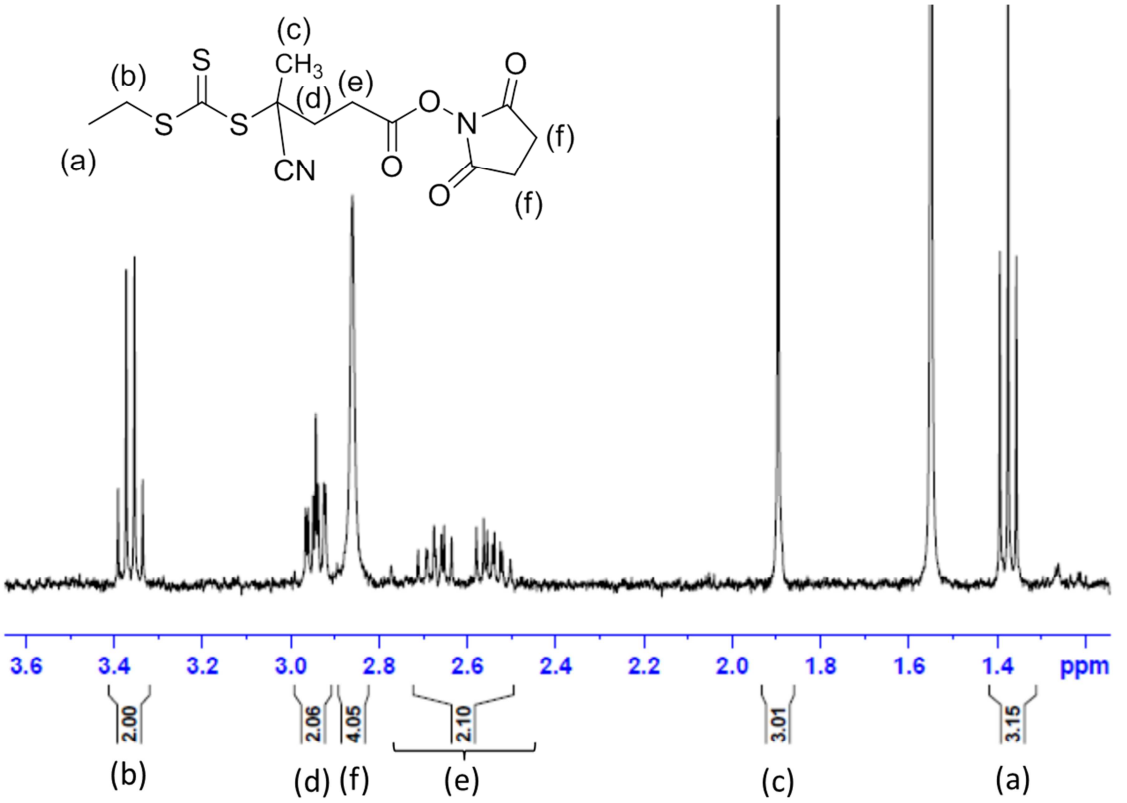

Figure S6. ^{1}H-NMR spectrum of the succinimide-functionalized ECT (NHS-ECT) in MeOH-d_4.

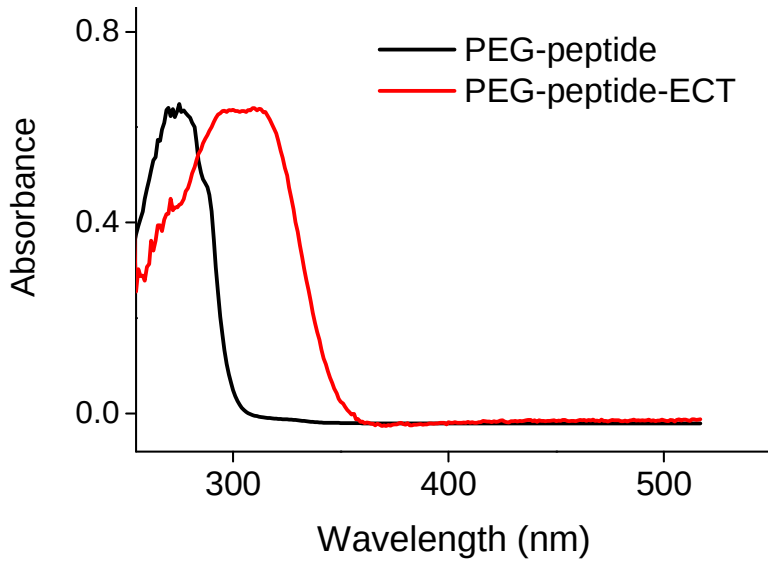

Figure S7. UV-vis spectroscopy characterization of the purified ECT functionalized PEG-peptide. The optical absorbance at 320 nm is consistent with conjugation of ECT onto PEG-peptide.

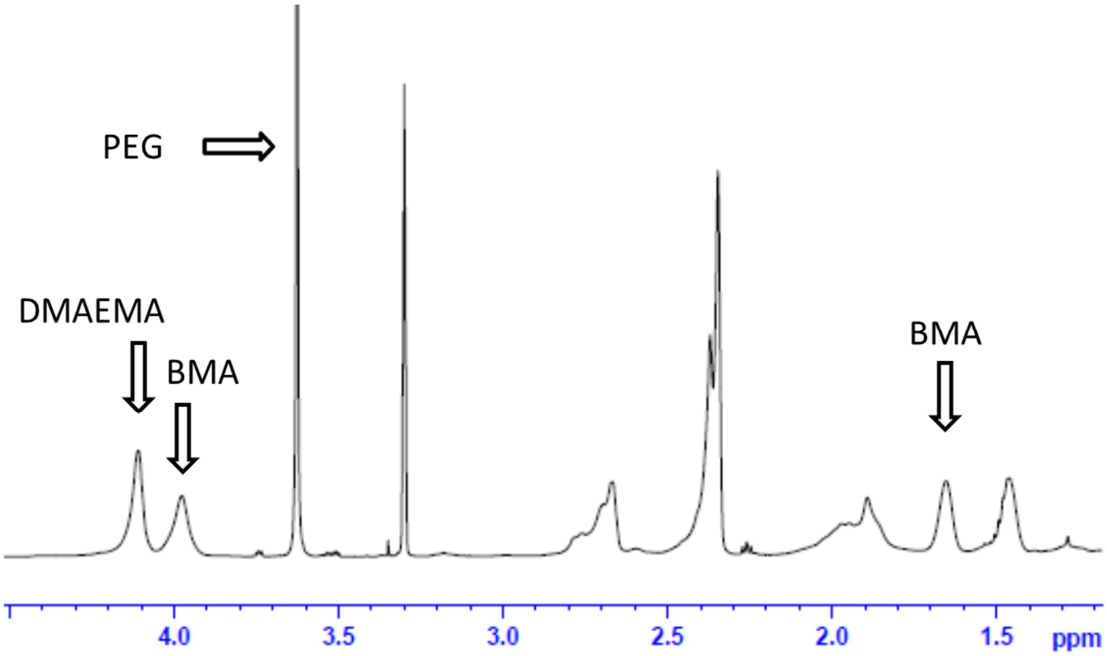

Figure S8. ^{1}H-NMR spectrum of PEG-pep-pD-pDPB in MeOH-d_4.

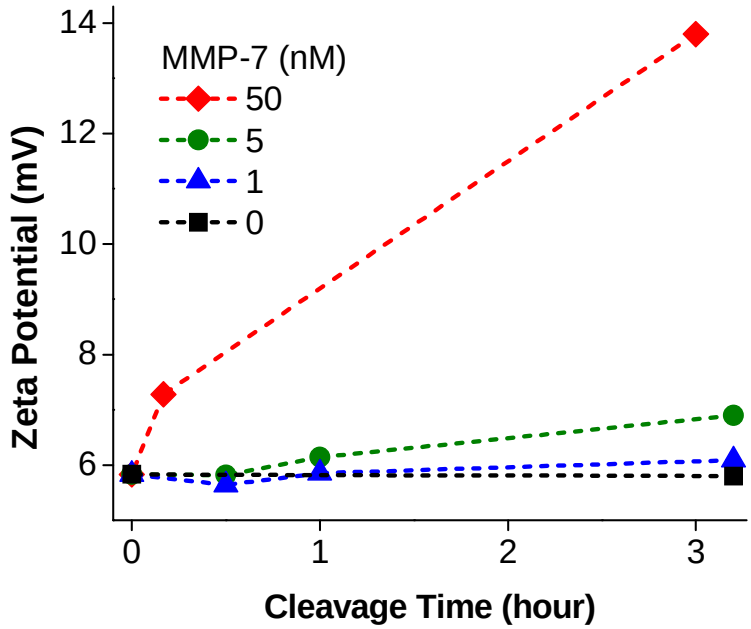

Figure S9. MMP-7 concentration dependent physicochemical switch activity in PAT-SPNs (0, 1, 5, and 50 nM MMP-7). Nanocarrier ζ-potential increased from +5.83 to +13.8 mV over 3 h of treatment with a metastasis-relevant MMP-7 concentration (50 nM, red) but not under MMP-7 levels corresponding to normal tissues (blue and green) in the presence of 50 µM of Zn^{2+}. ζ-potential after 3 h treatment of MMP-7 at 5 nM concentration increased from +5.83 to +6.90 mV (green) and from +5.83 to +6.09 mV at 1 nM concentration (blue). No addition of MMP-7, but with 50 µM of Zn2+, is reported here as 0 nM MMP.

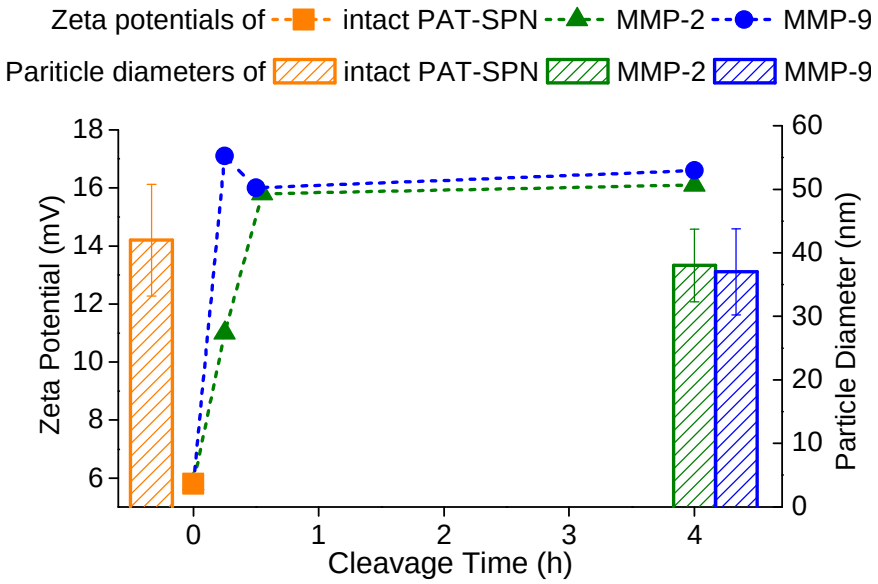

Figure S10. Responsiveness of PAT-SPNs to MMP-2 and MMP-9. Following treatment with 50 nM MMP-2, PAT-SPN zeta potential increased from +5.8 to +15.8 mV (green line) and particle diameter decreased by 4 nm (green column). Following treatment with 50 nM MMP-9, zeta potential increased to +16.0 mV (blue line) and particle diameter decreased by 5 nm (blue column). The zeta potential responses were rapid, occurring in less than 0.5 h of treatment. These changes are consistent with proteolytic cleavage of the VPLSLYSG and the subsequent shedding of the PEG corona.

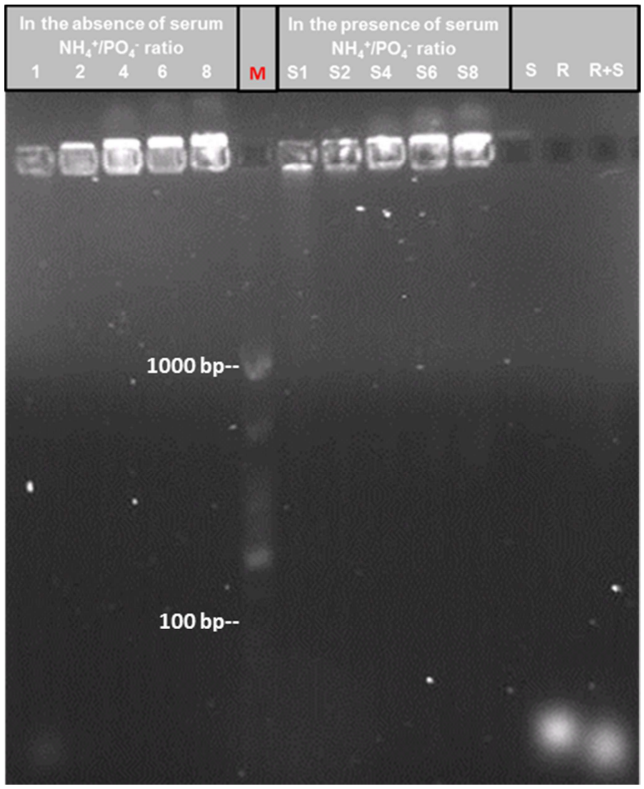

Figure S11. Serum stability of siRNA loaded into PAT-SPN was assessed using agarose gel electrophoresis. siRNA was combined with PAT-SPN with N(+)/P(-) charge ratios of 1/1, 2/1, 4/1, and 8/1. Samples were mixed with no (left side) or with (middle) 40% serum. Control lanes were loaded with serum (S), siRNA (R), or siRNA in 40% serum (R+S) (right side). The absence of free nucleotide in the PAT-SPN lanes suggests effective protection of siRNA against serum-induced instability.

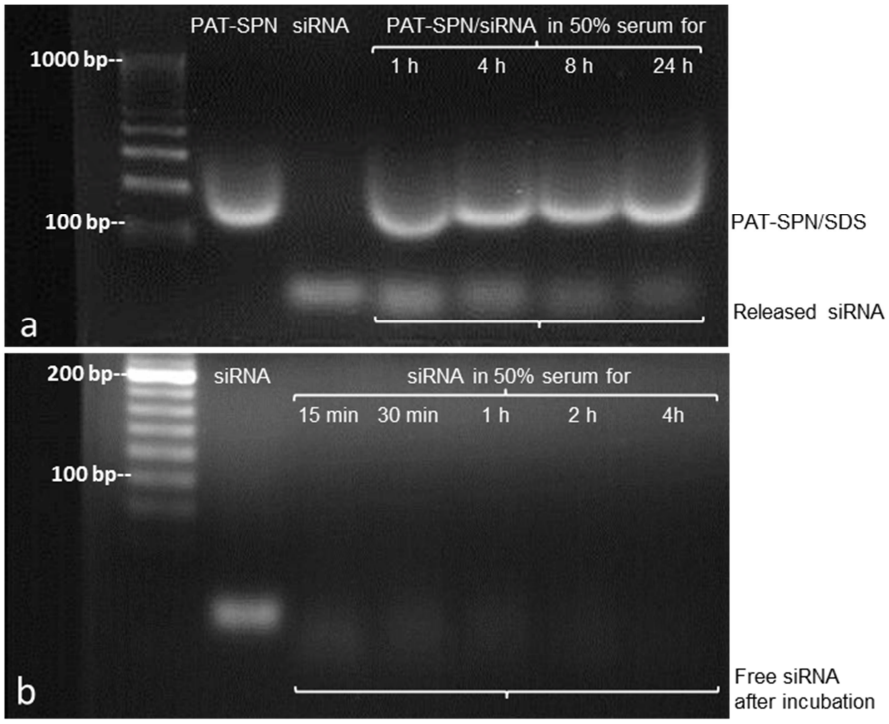

Figure S12. PAT-SPNs protect siRNA from (a) degradation, relative to (b) free siRNA in the presence of 50% serum at 37°C. (a) PAT-SPN were loaded with siRNA and incubated in 50% serum at 37°C. At the end of the incubation, siRNA was released from the PAT-SPN by the addition of 1% SDS. From left to right: molecular weight ladder; PAT-SPN alone (no siRNA)+SDS; siRNA alone (no PAT-SPN); PAT-SPN+siRNA incubated for 1 hr, 4 hrs, 8 hrs, 24 hrs, then SDS added. The relative persistence of band intensity for released siRNA suggests effective protection by PAT-SPN from nuclease activity in serum (relative to unprotected siRNA plus serum). (b) From left to right: molecular weight controls; siRNA in the absence of serum; siRNA incubated in 50% serum at 37°C for 0.25 hr, 0.5 hr, 1 hr, 2 hrs, 4hrs. The dimunition of band intensity for free siRNA suggests rapid degradation of unprotected siRNA by nucleases in serum.

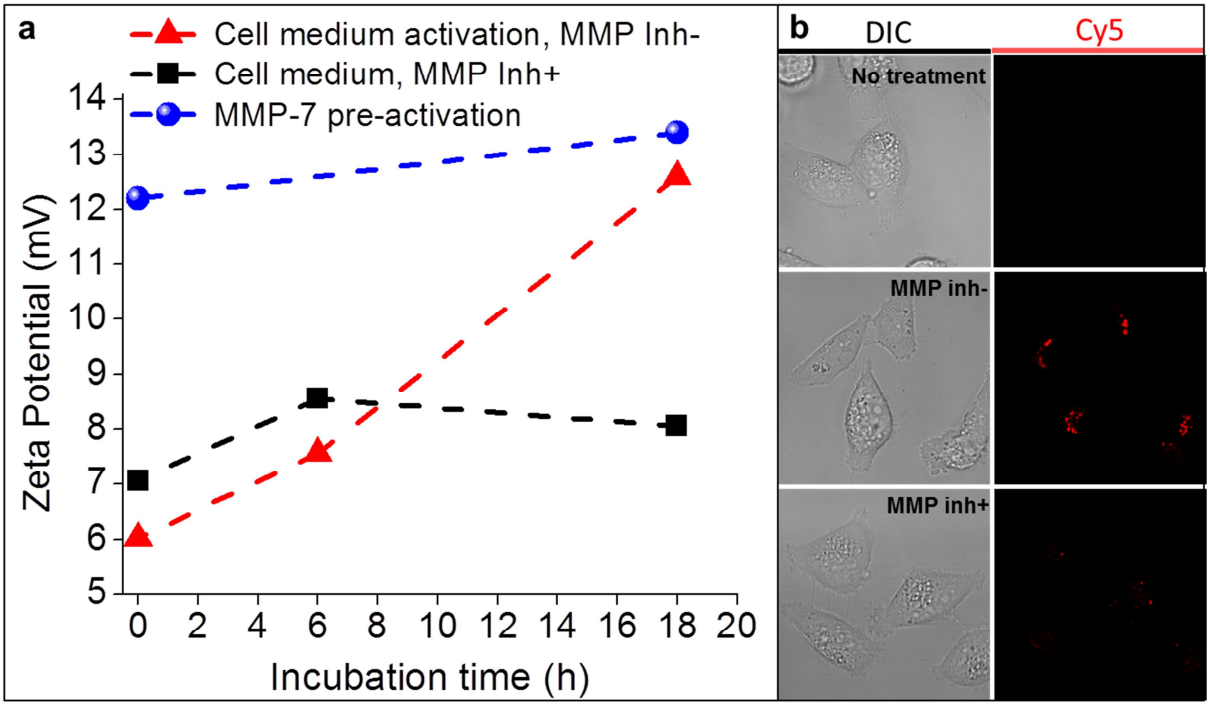

Figure S13. Activation of PAT-SPNs by MMPs endogenously produced by MDA-MB-231 breast cancer cells as analyzed by zeta potential measurement and confocal microscopy. **(a)** Following incubation in MDA-MB-231 conditioned media, the ζ-potential of PAT-SPN/DNA (N(+)/P(-)=6, 0.5 mg/mL polymer) increased from +6.0 to +12.6 mV (red line) in 18 h and reached values comparable to that induced by treatment with exogenous MMP-7 (blue line). On the contrary, the zeta potential was stable in the conditioned media supplemented with pan-MMP inhibitor (inh+) GM6001 (black line). **(b)** Cellular internalization of PAT-SPN/DNA^{Cy5} (N(+)/P(-)=6, 50 nM DNA^{Cy5}, 0.02 mg/mL polymer) was reduced in tissue culture upon addition of a broad spectrum MMP inhibitor, suggesting that there is a correlation between local MMP activity and degree of PAT-SPN cellular internalization. Microscope settings were adjusted in each experiment to achieve sufficient contrast in the brightest sample and were thereafter held constant for all other samples imaged.

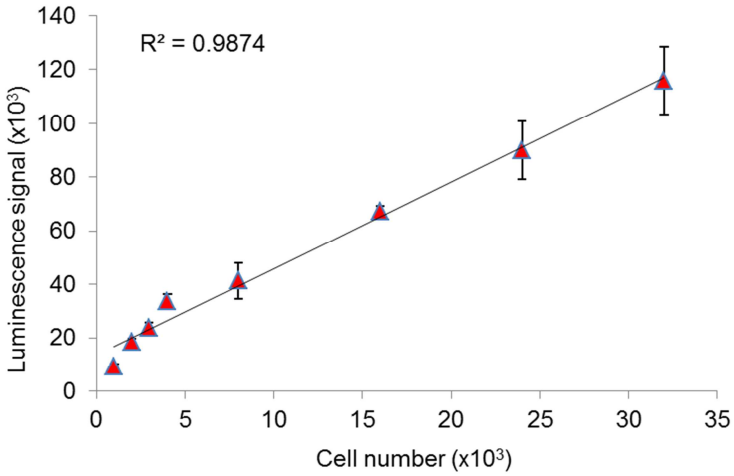

Figure S14. Correlation between cell number and luciferase bioluminescence intensity in R221A-luc tumor cells. A positive linear correlation of the R221A-Luc cell number with the luciferase signal was observed.